JTTEE5 19:510–516
DOI: 10.1007/s11666-009-9364-8
1059-9630/$19.00 © ASM International

Chemical Vapor Deposition and Atomic Layer Deposition of Coatings for Mechanical Applications

G.L. Doll, B.A. Mensah, H. Mohseni, and T.W. Scharf

(Submitted April 27, 2009; in revised form July 1, 2009)

Chemical vapor deposition (CVD) of films and coatings involves the chemical reaction of gases on or near a substrate surface. This deposition method can produce coatings with tightly controlled dimensions and novel structures. Furthermore, the non-line-of-sight-deposition capability of CVD facilitates the coating of complex-shaped mechanical components. Atomic layer deposition (ALD) is also a chemical gas phase thin film deposition technique, but unlike CVD, it utilizes "self-limiting" surface adsorption reactions (chemisorption) to control the thickness of deposited films. This article provides an overview of CVD and ALD, discusses some of their fundamental and practical aspects, and examines their advantages and limitations versus other vapor processing techniques such as physical vapor deposition in regard to coatings for mechanical applications. Finally, site-specific cross-sectional transmission electron microscopy inside the wear track of an ALD ZnO/ZrO_2 8 bilayers nanolaminate coating determined the mechanisms that control the friction and wear.

Keywords atomic layer deposition, chemical vapor deposition, protective coatings, tribology

1. Introduction

Chemical vapor deposition (CVD) is a process employing chemical reactions of gases near substrates for the purposes of depositing various materials. In a typical CVD process, the substrate is exposed to one or more volatile precursors, which react and/or decompose on the surface to produce the deposited material. Usually, volatile byproducts are also produced, which are removed by gas flow through the reaction chamber. CVD is a very versatile process used in the production of coatings, powders, fibers, and monolithic parts. It is possible to produce with CVD almost any metallic or nonmetallic element, including carbon and silicon, as well as compounds such as carbides, nitrides, borides, oxides, intermetallics, and many others.

This article is an invited paper selected from presentations at the 2009 International Thermal Spray Conference and has been expanded from the original presentation. It is simultaneously published in *Expanding Thermal Spray Performance to New Markets and Applications: Proceedings of the 2009 International Thermal Spray Conference*, Las Vegas, NV, USA, May 4-7, 2009, Basil R. Marple, Margaret M. Hyland, Yuk-Chiu Lau, Chang-Jiu Li, Rogerio S. Lima, and Ghislain Montavon, Ed., ASM International, Materials Park, OH, 2009.

G.L. Doll, The Timken Technology Center, Canton, OH; and **B.A. Mensah, H. Mohseni,** and **T.W. Scharf**, The University of North Texas, Denton, TX. Contact e-mail: gary.doll@timken.com.

CVD is widely used in the semiconductor industry, as part of the semiconductor device fabrication process, to deposit various films including: polycrystalline, amorphous and epitaxial silicon, silica, silicon germanium, tungsten, silicon nitride, silicon oxynitride, titanium nitride, and various high-k dielectrics (Ref 1). CVD is used in industrial applications to produce synthetic diamonds (Ref 2), boron nitride (Ref 3), and carbon/carbon composites (Ref 4) for example.

Since the CVD process uses gases as reactants, it has several distinct advantages over most other deposition processes. For example, CVD is not a line-of-sight process as are most other plating/coating processes. It has the ability to penetrate porous bodies, form deposits in blind holes, and the inside diameters of tubes. CVD is extraordinarily versatile since it can be used to deposit any element or compound. Exceptionally high-purity (typically 99.99 to 99.999%) deposits can be made with densities equivalent to the theoretical bulk material values. By combining the proper precursors, materials can be formed well below their melting point. Coatings deposited by CVD are conformal and near net shape, and since many parts can be coated at the same time, CVD can be a very economical production process.

On the other hand, there are some important disadvantages that CVD has in regard to other processes such as physical vapor deposition (PVD). Chemical and safety hazards usually exist that are caused by the use of toxic, corrosive, flammable, and/or explosive precursor gases. Second, it can be very difficult to deposit multicomponent materials with well-controlled stoichiometries since multiple precursors typically have different vaporization rates.

Atomic layer deposition (ALD) was first developed in the 1970s for thin film electroluminescent flat panel

displays (Ref 5, 6). Since then ALD has found niche applications in microelectronics, optics, protective coatings, and gas sensors (Ref 7-9). The ALD process is a surface reaction controlled variant of the CVD technique. It uses the sequential introduction of gaseous precursors and selective surface chemistry to achieve atomic scale-controlled growth at reduced temperatures ranging from 100 to 400 °C. Because of the self-limiting nature of ALD, the coatings have very uniform thickness even if the flux of vapor is distributed nonuniformly over the surface. This efficient transport of material into confined spaces at low pressure, and sequential introduction of reactants leads to excellent control of coating thickness and coverage of high aspect ratio structures. This attribute allows ALD to be ideally suited for coating shadowed surfaces on the underside of moving mechanical assemblies such as microelectromechanical systems (MEMS) (Ref 10) and rolling element bearings (Ref 11).

2. CVD Processes

Thermally activated CVD (TACVD) describes a process where the chemical reactions are initiated by thermal energy using inorganic chemical precursors. This process can also be subdivided according to the pressure range of the deposition. For example, atmospheric pressure CVD, low-pressure CVD, and ultrahigh vacuum CVD are performed at atmospheric pressures, low pressure (0.01 to 1.33 kPa), and ultrahigh vacuum (less than 10 to 4 kPa), respectively. TACVD is commonly used to fabricate semiconductors, dielectrics, and metallic films for microelectronics, optoelectronics, and energy conversion devices. It is also used to produce ceramics such as SiC, TiC, B_4C, TiN, BN, Si_3N_4, TiB_2, $MoSi_2$, and Al_2O_3 in the form of coatings to protect components against chemical diffusion, wear, friction, oxidation, and corrosion. TACVD is used to produce aluminized bonding layers between the Ni-based superalloys and the ceramic top coats (e.g., Y_2O_3-ZrO_2) of turbine blades. It is also used to produce silica optical fibers, B and SiC monofilament fibers, and coatings on fibers used in metal matrix, ceramic matrix, or carbon/carbon composites.

Plasma-enhanced CVD (PECVD) uses electron energy as the activation method to enable deposition to occur at lower temperatures with higher rates than TACVD. PECVD is generally limited to low-temperature applications that cannot be met by TACVD. Examples of materials produced by PECVD include diamond (microwave, RF, and hot-filament activation), diamond-like carbon films (DLC) for optical and tribological applications, and nitrides like TiN and AlN for tool coatings and light emitting applications.

Photo-assisted CVD (PACVD) is a process that relies on the absorption of light to raise the substrate temperature and cause thermal decomposition of the precursor in the gas phase and/or on the substrate surface.

Metalorganic CVD (MOCVD) is a variant of CVD classified according to its use of metalorganic precursors. MOCVD was developed and used almost exclusively in the growth of epitaxial III-V, II-VI, and IV-VI semiconductors for optoelectronic applications. Other lesser known and utilized CVD processes include aerosol-assisted CVD, flame-assisted CVD, and electrochemical vapor deposition.

3. ALD Processes

ALD has many alternative names such as atomic layer epitaxy, atomic layer CVD, atomic layer growth, and molecular layering. Plasma-assisted ALD is another process that utilizes plasma sources in conjunction with ALD where, for example, atomic H reacts away the halogen (or organometallic precursor) in the *B* reaction and the exposed surface is reactive for next dose of the *A* reactant. Plasmas can also be used to make binary materials. The technological importance of ALD as a deposition technique is only beginning to be appreciated by the microelectronics industry as the pool of film growth techniques, that is able to keep pace with the diminution of device dimensions, shrinks. Currently, ALD is still very much confined to research laboratories. However, it is up-scalable and thus projected to replace PVD, and in some cases CVD, as device length scales continue to diminish and film quality, uniformity, conformality, and thickness become more critical.

4. CVD Process Physics

Choy describes the seven key steps in a CVD film growth process (Ref 1). They are illustrated in Fig. 1 and listed below.

1. Generation of active gaseous reactant species.
2. Transport of gaseous species into the reaction chamber.
3. Gaseous reactants undergo gas phase reactions forming intermediate species:
    a. At temperatures greater than the decomposition temperature of the intermediate species inside the reactor, homogeneous gas phase reactions can occur and form powders and volatile by-products in the gas phase.
    b. At temperatures less than the dissociation temperature of the intermediate phase, diffusion/convection of the intermediate species across a thin boundary layer near the substrate surface occurs. The intermediate steps subsequently undergo steps 4 to 7.
4. Absorption of gaseous reactants onto the heated substrate surface.
5. Deposits will diffuse along the heated substrate surface forming a crystallization center and growth of the film.

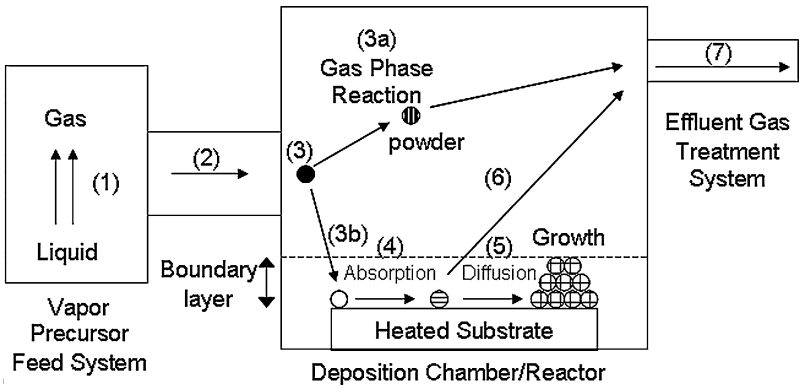

Fig. 1 Schematic illustration of the seven key steps in a CVD process

6. Gaseous by-products are removed from the boundary layer through diffusion or convection.
7. Unreacted gaseous precursors and by-products are transported away from the deposition chamber.

A thorough knowledge of a CVD process requires an understanding of the thermodynamics and kinetics involved. The feasibility of a CVD reaction can be determined from a calculation of the thermodynamic equilibrium at a given set of processing conditions. The Gibbs free energy of the reaction (ΔG_r) is the difference between the free energy of formation (ΔG_f) of the reactants and the products,

$$\Delta G_r = \Delta G_f^{prods} - \Delta G_f^{reacts} \quad \text{(Eq 1)}$$

At a temperature T,

$$\Delta G_f^{\circ}(T) = \Delta H_f^{298} + \int_{298}^{T} C_p dT - TS_0^{298} - \int_{298}^{T} \left(\frac{C_p}{T}\right) dT \quad \text{(Eq 2)}$$

where the free energy of formation is a function of the standard enthalpy of formation (ΔH_f^{298}) and entropy (S_0^{298}) at 298 K, and the heat capacity (C_p). If ΔG_r is negative, a reaction will occur, and no reaction will occur if ΔG_r is positive. If there are several possible reactions that are thermodynamically feasible, the reaction with the most negative ΔG_r value will dominate because it has the most stable reaction products. The equilibrium constant, K, can be determined from

$$K = \exp(-\Delta G_f / RT) \quad \text{(Eq 3)}$$

where R is the gas constant and T is the deposition temperature. Once K is known, the partial pressure of the gaseous species and products can be calculated using the law of mass action.

CVD is usually a nonequilibrium process involving chemical reactions in the gas phase, on the substrate surface, chemisorption, and desorption. The overall reaction rate is limited by the slowest reaction step. Whereas limited data exist on the surface reaction mechanisms, activation, and absorption energies, CVD kinetics are typically determined by experimentally measuring the deposition rates and matching them to the possible rate-limiting reactions. For example, consider the synthesis of TiB_2 coatings according to the reaction:

$$TiCl_4 + 2BCl_3 + 5H_2 \xrightarrow{T} TiB_2 + 10HCl \quad \text{(Eq 4)}$$

Choy (Ref 1) found that the deposition rate as a function of temperature is in compliance with the Arrhenius law:

$$\text{Dep Rate} = A \exp(-E_a/RT) \quad \text{(Eq 5)}$$

where A is a constant, E_a is apparent activation energy, R is the gas constant, and T is the deposition temperature. For $1050 < T < 1350$ °C, the deposition rate increases rapidly in an exponential manner with $E_a \sim 144$ kJ/mol. This indicates that the rate-limiting mechanism is surface kinetics since it depends strongly upon the deposition temperature. For $1350 < T < 1450$ °C, the deposition rate decreases due to the depletion of reactants and/or increase in the rate of desorption, and E_a decreases to about 30 kJ/mol. For $T > 1450$ °C, homogeneous gas phase reactions begin to occur leading to particle formation in the gas phase and an interruption in the growth of the TiB_2 coatings.

Most CVD processes including TACVD, PECVD, and PACVD operate in the surface kinetic limited regime because there is an abundance of reactants near the substrate surface undergoing slow chemical reactions with negligible local variations of reactant concentrations.

5. ALD Process Physics

ALD is also a chemical gas phase thin film deposition technique, but unlike CVD, it utilizes ''self-limiting'' surface adsorption reactions (chemisorption) to control the thickness of deposited films. In CVD,

$$\text{surface} + X + Y \rightarrow \text{surface}{:}XY \quad \text{(Eq 6)}$$

where X and Y precursors (reactants) enter into the chamber as gases in which they react on a heated substrate to produce a film and/or can also react just above surface

to produce a film. ALD breaks up the CVD chemical reaction into two self-limiting ''half reactions,'' *A* and *B*:

$$A \text{ reaction:} \quad \text{surface} + X \rightarrow \text{surface:}X \qquad \text{(Eq 7)}$$

$$B \text{ reaction:} \quad \text{surface:}X + Y \rightarrow \text{surface:}XY \qquad \text{(Eq 8)}$$

Each ''half reaction'' is sequenced one at a time followed by a purge cycle that pumps away any unreacted or excess reactant in the chamber. This allows for cycling of the half reactions: pulse *A*, purge *A*, pulse *B*, purge *B*, and then repeated for *N* amount of cycles. This sequencing will result in thin film deposition. ALD cycle times range from subsecond to many seconds depending on sample geometry and chemistry. In the well-studied case of Al_2O_3 deposition, trimethylaluminum (TMA) and DI H_2O are the metal and oxidant precursors, respectively (Ref 9). The surface alternates between a methyl-terminated and a hydroxyl-terminated surface after TMA and DI H_2O pulses, respectively. If the substrate is hydroxylated silicon, the following half reactions (*A* and *B*) occur at the first TMA and DI H_2O pulses:

$$A \text{ reaction:} \quad \text{Si:OH}^* + \text{Al(CH}_3)_3 \rightarrow \text{Si:OAl(CH}_3)^* + \text{CH}_4(g) \qquad \text{(Eq 9)}$$

$$B \text{ reaction:} \quad \text{Si:OAl(CH}_3)^* + \text{H}_2\text{O} \rightarrow \text{Si:OAlOH}^* + \text{CH}_4(g) \qquad \text{(Eq 10)}$$

where * indicates surface species.

Because of self-limiting behavior of each *AB* ALD cycle, one can precisely control the thickness of film by performing a desired number of *AB* cycles, commonly referred to as growth per cycle (GPC). Other advantages of ALD films are conformality in high aspect ratio structures like pores, trenches, and buried surfaces, reaction temperatures are typically lower than corresponding CVD reactions, and the ability to investigate the nucleation chemistry of thin film deposition one layer at a time.

Figure 2 shows a hot-wall viscous flow ALD reactor that uses N_2 as the carrier and purge gas. The reactor design shown is similar to the ALD viscous flow reactor of Elam et al. (Ref 12). In the case of WS_2 deposition, a solid lubricant coating applied to rolling element bearings, the WF_6 and H_2S precursors were injected into the carrier gas stream using pneumatically operated valves (Ref 11). Their pulse times were 2 s and their purge times were 5 and 25 s for WF_6 and H_2S, respectively, at a total pressure of 267 Pa (2 Torr). Diethyl zinc was used as a growth catalysis. Nitrogen gas was supplied via a mass flow controller with a throughput of 50 sccm on the reactant lines. A dry pump was used to reach a base pressure of approximately 0.67 Pa (5 mTorr).

Limitations of ALD include the long duration to grow a thick film (*AB* GPC are small ≈1 Å), no selective deposition (presently), growth chemistry is very different from nucleation chemistry, and precursor vapor pressure limits the types of reactants (hence, compounds that can be synthesized). For example, in the latter, there are currently no known DLC solid lubricant thin film precursors that meet the requirements of ALD.

ALD precursors must be volatile and thermally stable to be converted successfully to the gas phase, need to reach surface saturation and not multilayer adsorption. ALD surface reactions need to be thermodynamically favorable (large—ΔG_r), and the more reactive the precursor, the lower the reaction temperature, while the larger the molecular precursor, the lower the GPC. In the case of nonmetal ALD precursors, like DI H_2O and NH_3, they make up only a small fraction of precursors, unlike metal organics there is no volatility or thermal stability issues, they react at reasonable temperatures <500 °C, and they form suitable surface species for the second half-reaction to react.

ALD's unique features allow the growth of highly conformal films with accurate thickness over large areas. Ritala and Leskelä (Ref 7) list other benefits of ALD including:

- Large-batch compatibility,
- Insensitivity to nonuniform precursor vaporization rate,
- Good reproducibility,
- Straightforward scale-up (i.e., film thickness is only dependent on the number of deposition cycles),

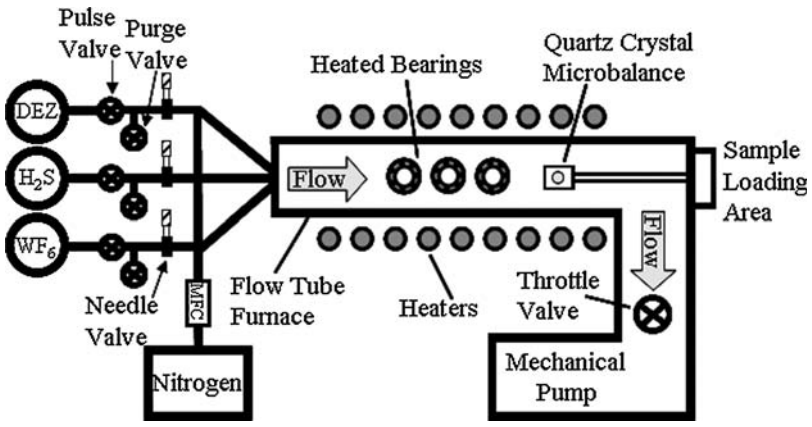

Fig. 2 Schematic of viscous flow reactor used to grow ALD WS_2 coatings on rolling element bearings (after Ref 11 and 12)

- Composition control down to atomic level,
- Capability to produce sharp interfaces and superlattices,
- Lack of gas phase reactions favors use of highly reactive precursors and leads to effective material utilization,
- Low processing temperatures, and
- Capability to prepare multilayer structures in a continuous processing due to relatively wide processing temperature window.

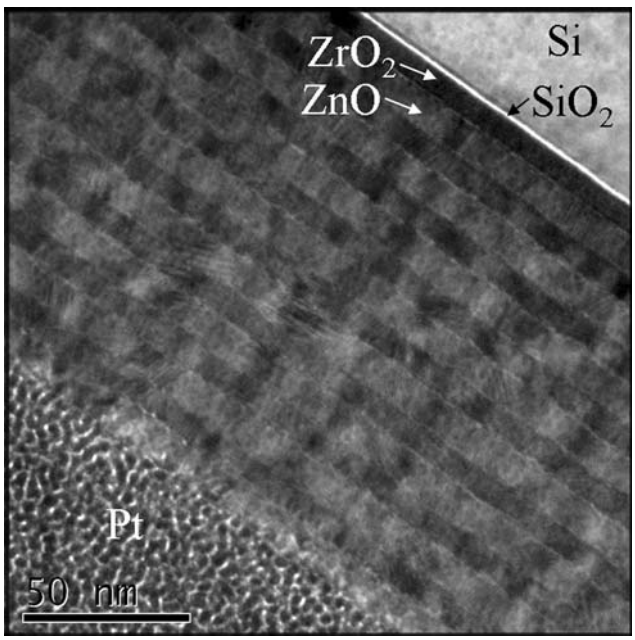

Fig. 3 Cross-sectional transmission electron micrograph of ALD ZnO/ZrO_2 8 bilayer nanolaminate coating grown at 200 °C. Platinum was deposited to protect the coating from cross-sectional milling

6. Example of ALD Coating for Mechanical Applications

Figure 3 shows a bright field cross-sectional transmission electron micrograph (XTEM) of a ~140 nm thick ALD ZnO/ZrO_2 8 bilayers nanolaminate coating on silicon substrate with its ~2 nm thick native SiO_2 layer. To protect the region of interest from ion beam damage prior to FIB milling, electron and ion beam-assisted Pt were first deposited. It is evident from the image that distinct and sharp interfaces exist between the crystalline ZnO (~10 nm thick) and ZrO_2 layers (~7 nm thick). Both layers exhibit nanocolumnar grains growing to layer thickness. The corresponding x-ray diffraction (XRD) of this nanolaminate at room temperature and ex situ annealed at 400 °C for 2 h is shown in Fig. 4. XRD for both scans confirms both hexagonal ZnO (wurtzite structure) and tetragonal ZrO_2 are crystalline with each bilayer exhibiting (0002) and (101) texture, respectively. The (0002) texture, otherwise called c-axis orientation, is commonly observed in ZnO films because the c-plane perpendicular to the substrate normal is the most densely packed and thermodynamically preferred in the wurtzite structure. A (0002) texture has been shown to promote good tribological properties in pulsed laser-deposited ZnO, so promoting its growth in the nanolaminates is productive for tribological applications (Ref 13). Meanwhile, the relatively high-toughness ALD ZrO_2 should act as a load bearing layer (at moderate contract stresses) and as a pathway to dissipate energy to prevent cracking between the bilayers. In addition, Fig. 4 shows that ex situ

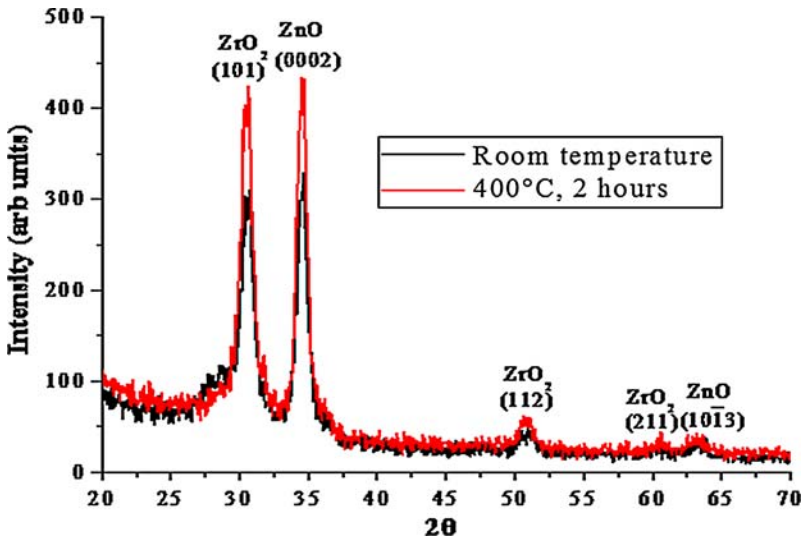

Fig. 4 X-ray diffraction of ALD ZnO/ZrO_2 8 bilayer nanolaminate coating at room temperature and ex situ annealed at 400 °C for 2 h

annealing the nanolaminate to 400 °C for 2 h resulted in no ZrO_2 tetragonal to monoclinic phase transformation and no ZnO (0002) or ZrO_2 (101) peak shifts or full-width at half maximum peak broadening, which suggest there was no grain growth or lattice strain due to annealing.

The steady-state friction coefficient of this nanolaminate coating was determined to be ~0.25, a relatively low value, at a maximum Hertzian contact stress of ~0.7 GPa sliding against a 440 C stainless steel ball at a linear speed of 2.2 cm/s for 10,000 unidirectional cycles. Mechanisms of solid lubrication were studied by FIB prepared cross-sectional cuts (parallel to the sliding direction) inside the center of the wear track to determine if there was any surface or subsurface deformation and its role in controlling the tribological behavior. Figure 5(a) shows the XTEM image of the worn 8 bilayers nanolaminate coating after the 10,000 cycles test. The image shows that only the top ZnO layer has experienced deformation among the 16 individual layers. Also shown is a nonuniform layer (up to ~10 nm thickness) just below the protective Pt layer. The arrow in the figure points to a region where this layer is absent and shows slight thinning (wear) of the ZnO layer. Figure 5(b) shows a magnified view of these top layers taken from the box located in Fig. 5(a). It is apparent that the nonuniform layer is amorphous which could either be from the native oxide, Fe_xO_y, on the 440 C stainless steel ball (adhesive wear) and/or this layer has undergone a stress-induced transformation from columnar structure to amorphous ZnO. Energy dispersive spectroscopy inside the TEM does not have the resolution to identify the phase(s) in this mechanically mixed (third-body) layer, and therefore x-ray photoelectron spectroscopy is planned. While the nanolaminate oxides are stable at high temperatures, this surface layer may not be and thus future high-temperature tribological testing is planned. There was no visible transfer film accumulated on the steel ball surface. Furthermore, no microcracks were observed among any of the layers even in the deformed top ZnO layer, which suggests that the bilayers were effective in dissipating the energy required to initiate a crack.

It is also possible that the crystalline to amorphous stress-induced transformation was accompanied by volume expansion due to less efficient atomic packing. The mixed amorphous-crystallite nature of this transformed layer makes it easy to accommodate interfacial shear. The plastic deformation process appears to be the continuous decrease in crystal size due to the applied cyclic stress until eventual amorphization. Hence, for this nanolaminate, the applied energy was being used to (a) transform the columnar grains to progressively smaller crystals and eventually to amorphous ZnO, and (b) in shearing the transformed ZnO layer across the surface to accommodate the sliding motion of the ball, i.e., the velocity accommodation mode is intrafilm shear.

Unlike most solid lubricants, such as graphite, DLC, and WS_2, oxides are thermodynamically stable compounds with minimal grain coarsening, and should perform well over a wide range of environmental conditions such as thermal cycling, as evident by the aforementioned 400 °C anneal shown in Fig. 4. Therefore, these lubricious oxide

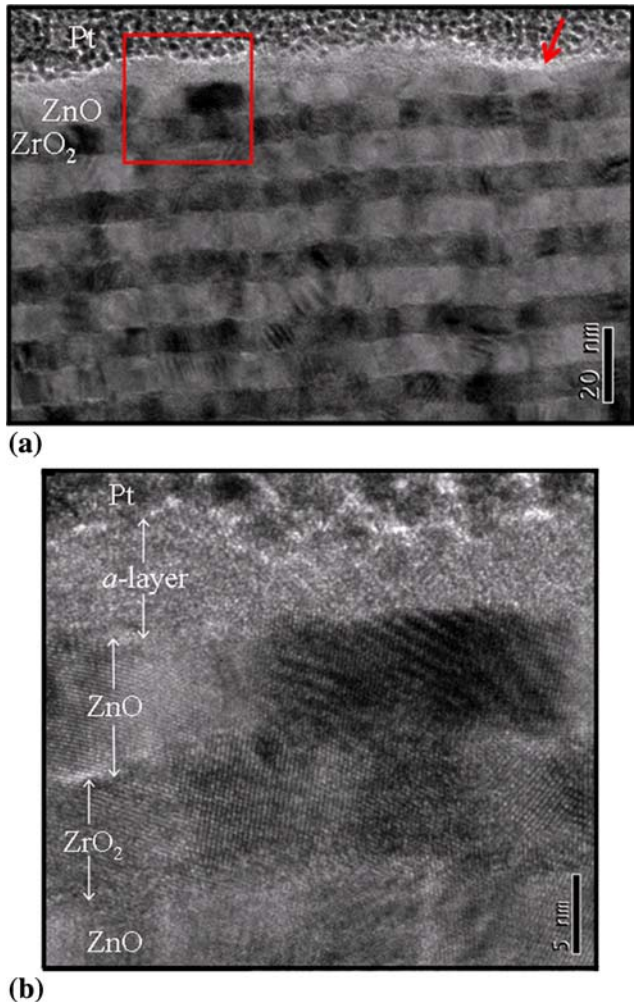

Fig. 5 Cross-sectional transmission electron micrograph of worn ALD ZnO/ZrO_2 8 bilayer nanolaminate coating at two magnifications. Box in (a) shows location of image in (b) and arrow points to worn ZnO. Platinum was deposited to protect the coating from cross-sectional milling

nanolaminate coatings are being targeted for high-temperature mechanical applications, such as in thrust ball bearings, and high-temperature vacuum rolling contact fatigue testing is planned.

7. Comparison of CVD and ALD with PVD

This section compares CVD and ALD to PVD techniques such as molecular beam epitaxy, sputtering, evaporation, and pulsed laser deposition. The undisputed advantage that CVD and ALD offer over PVD is the ability to coat complex geometries due to their nonline of sight process capabilities. Comparisons of other characteristics such as cost/part, complexity, environmental impact, compositional control, and deposition temperature are not as clear cut and depend upon the specifics of the application-driven process. For example, although

Table 1 Attribute comparison of CVD, ALD, and PVD processes (M = molecular beam epitaxy, S = sputtering, E = evaporation, P = pulsed laser deposition)

Attribute	CVD	ALD	M	S	E	P
Thickness uniformity	Good	Good	Fair	Good	Fair	Fair
Film density	Good	Good	Good	Good	Poor	Good
Step coverage	Vary	Good	Poor	Poor	Poor	Poor
Interface quality	Vary	Good	Good	Poor	Good	Vary
# of Materials	Fair	Fair	Good	Good	Fair	Poor
Low-temperature deposition	Vary	Good	Good	Good	Good	Good
Deposition rate	Good	Fair	Poor	Good	Good	Good
Industrial applicable	Good	Good	Fair	Good	Good	Poor

most CVD and PVD processes require a sophisticated reactor and vacuum system, there are some CVD (aerosol-assisted, flame-assisted, and electrochemical) and PVD processes that do not. Table 1 summarizes additional comparisons of some of the attributes of generalized CVD, ALD, and PVD processes.

8. Conclusions

CVD and ALD of films and coatings involve the chemical reaction of gases on or near a substrate surface. These non-line-of-sight methods can produce conformal and uniform coatings in extremely high aspect ratio and buried surfaces on nanostructures compared to PVD techniques. Moving mechanical assemblies, such as rolling element bearings and MEMS, must function reliably and predictably in device operation. The ongoing significant reduction in the dimensions of these devices and components increases dramatically the influence of dynamic surface interactions, including rubbing and/or sliding-induced friction and wear, on service performance and reliability in applications. CVD and ALD deposition of hard and solid lubricant phases, such as ZrO_2 and ZnO, respectively, can mitigate these issues by providing nanoscale conformality and uniformity of coatings on buried surfaces and interfaces. Furthermore, incorporation of plasma excitation in both techniques to fully or partially drive chemical reactions reduces material limitations in many cases.

A case study showed that a ALD ZnO/ZrO_2 8 bilayers nanolaminate coating exhibited low friction and wear in sliding and potentially in rolling contacts. Evidence of a friction-reducing surface layer was determined with XTEM inside the wear track. Interfacial sliding with this friction-induced surface layer aids in shear accommodation and prevents brittle fracture. The formation of this compliant surface layer in ZnO/Al_2O_3 nanolaminates was related to the synergistic effect of: (a) a low surface energy (0002) ZnO texture, (b) small enough grain size ($<$20 nm), and (c) a top ZnO layer thickness that is sufficient to prevent ZrO_2 from being mixed into the deformed layer. Therefore, it is feasible to generate lubricious oxides through microstructural control at the nanometer level.

Acknowledgments

The Timken Company is acknowledged for support of this work and permission to publish. This work was supported by the National Science Foundation (Grant No. CMMI-0700828).

References

1. K.L. Choy, Chemical Vapor Deposition of Coatings, *Prog. Mater. Sci.*, 2003, **48**, p 57-170
2. W. Wang, T. Moses, R.C. Linares, J.E. Shigley, M. Hall, and J.E. Butler, Gem-Quality Synthetic Diamonds Grown by a Chemical Vapor Deposition (CVD) Method, *Gems Gemol.*, 2003, **39**, p 268-283
3. M.J. Rand and J.F. Roberts, Preparation and Properties of Thin Film Boron Nitride, *J. Electrochem. Soc.*, 1968, **115**, p 423-429
4. G. Savage, *Carbon Carbon Composites*, Springer, New York, 1993, p 85-113
5. T. Suntola and J. Anston, Method for Producing Compound Thin Films, U.S. Patent 4,058,430, 1977
6. T. Suntola and J. Hyvärinen, Atomic Layer Epitaxy, *Annu. Rev. Mater. Sci.*, 1985, **15**, p 177-195
7. M. Ritala and M. Leskelä, Atomic Layer Deposition, *Handbook of Thin Films*, Vol 1, H.S. Nalwa, Ed., Academic Press, San Diego, 2002, p 103-159
8. S.M. George, A.W. Ott, and J.W. Klaus, Surface Chemistry for Atomic Layer Growth, *J. Phys. Chem.*, 1996, **100**, p 13121-13131
9. R.L. Puurunen, Surface Chemistry of Atomic Layer Deposition: A Case Study for the Trimethylaluminum/Water Process, *J. Appl. Phys.*, 2005, **97**, p 121301-121352
10. T.W. Scharf, S.V. Prasad, M.T. Dugger, P.G. Kotula, R.S. Goeke, and R.K. Grubbs, Growth, Structure, and Tribological Behavior of Atomic Layer-Deposited Tungsten Disulphide Solid Lubricant Coatings with Applications to MEMS, *Acta Mater.*, 2006, **54**, p 4731-4743
11. T.W. Scharf, D.R. Diercks, B.P. Gorman, S.V. Prasad, and M.T. Dugger, Atomic Layer Deposition of Tungsten Disulphide Solid Lubricant Nanocomposite Coatings on Rolling Element Bearings, *Tribol. Trans.*, 2009, **52**, p 284-292
12. J.W. Elam, M.D. Groner, and S.M. George, Viscous Flow Reactor with Quartz Crystal Microbalance for Thin Film Growth by Atomic Layer Deposition, *Rev. Sci. Instrum.*, 2002, **73**, p 2981-2987
13. J.S. Zabinski, J.H. Sanders, J. Nainaparampil, and S.V. Prasad, Lubrication Using a Microstructurally Engineered Oxide: Performance and Mechanisms, *Tribol. Lett.*, 2000, **8**, p 103-116